

# Period of Efficient Underwater Hull Cleaning

Rifqi Al Baihaqi Wijaya<sup>1</sup>, Achmad Baidowi<sup>2</sup>, Sunarsih<sup>3\*</sup>

(Received: 4 December 2025 / Revised: 8 December 2025 / Accepted: 8 December 2025 / Available Online: 10 December 2025)

**Abstract**—Biofouling is a collection of unwanted living organisms on surfaces submerged in water. Biofouling is a complex occurrence caused by various physical and environmental factors that can be overcome by regular hull cleaning. The main purpose of underwater hull cleaning is to remove dirt and restore propulsion efficiency. Another benefit of hull cleaning against biofouling is to restore or rejuvenate the effectiveness of antifouling paint. This study aims to determine the extent of the effect of periodic hull cleaning on the underwater area, where the results can be used to determine the most efficient period for periodic hull cleaning and the percentage of fuel that can be saved by performing periodic underwater cleaning. The effect of biofouling can be predicted by conducting simulations using Computational Fluid Dynamics (CFD) with several variations in hull roughness. The results of the CFD simulation show that the increase in resistance with the largest surge occurs in the 18th period with an average increase of 5.8%. Therefore, the effective time to perform underwater hull cleaning is in the 18th period. Performing underwater hull cleaning in the 18th period can save fuel consumption by up to 5.8%.

**Keywords**—Biofouling, Underwater Hull Cleaning, Resistance, Computation Fluid Dynamics

\*Corresponding Author: sunarsih@its.ac.id

## I. INTRODUCTION

**S**hipping is a very important method of transportation, commensurate with the increasing importance of and dependence on shipping using sea transportation. However, technological improvements and advances in marine technology have brought several problems for the industry due to increased fuel consumption, which damages the environment and reduces company revenues [7].

The attachment and growth of living organisms on surfaces exposed to aquatic environments is defined as fouling. The formation of biofouling communities occurs through a process in which colonization of new surfaces occurs as a result of succession through several different stages (Egan, 2001) [8]. Biofouling on the hull surfaces of ships in contact with seawater is the main cause of several technical and economic problems in the shipping industry [2].

Although shipping is slightly more environmentally friendly than other modes of transportation, ships emitted 870 million tons of CO<sub>2</sub> in 2007, equivalent to 2.7% of total CO<sub>2</sub> emissions that year [6]. Based on resistance theory, biofouling on the hull and keel of ships can increase fuel consumption [4]. Fouling on the hull below the waterline can also mean increased fuel costs [3].

Biofouling attached to the hull of a ship can reduce a ship's power by up to 86% at cruising speed. Even relatively light fouling caused by diatom algae can result in a reduction of 10% to 16% [5]. Fuel consumption can increase by up to 40% unless preventive measures are taken to prevent fouling. To minimize these [12]. Factors to consider when selecting an antifouling system are defined as follows: expected dry-docking period, ship speed, ship operating profile, ship type, and legal requirements [12].

The main purpose of cleaning the underwater hull of a ship is to remove dirt and restore propulsion efficiency. Another benefit of cleaning the hull of a ship against biofouling is to restore or rejuvenate the effectiveness of anti-fouling paint [10]. Hull cleaning procedures to restore ship performance are categorized into two main approaches, namely dry-docking cleaning and underwater cleaning, which involves personnel scrubbing the hull surface while the ship is safely moored at the dock [9]. However, the main drawbacks of this method are the high docking and paint repair costs, long docking cycles, and severe pollution. Another reason this method is difficult is the difficulty of coordinating ship sailing schedules [14].

The problem raised in this research is about when is the right time to clean the hull of the underwater area and how the effect of biofouling at each period on the resistance of the ship, especially the drag coefficient simulated with the help of Computational Fluid Dynamics (CFD). Where the results can be used as a reference in ship maintenance, especially in the underwater hull area.

## II. METHOD

### A. Biofouling Growth Identification

At this stage, the growth of biofouling was identified through experiments using flat plates measuring 10 cm long x 10 cm wide x 0.3 cm high, which were immersed in the waters of the Madura Strait [11]. After collecting the data from the flat plate

---

Rifqi Al Baihaqi Wijaya, Department of Marine Engineering Institut Teknologi Sepuluh Nopember ITS, Surabaya 60111, Indonesia

Achmad Baidowi, Department of Marine Engineering Institut Teknologi Sepuluh Nopember ITS, Surabaya 60111, Indonesia.  
Email: achmad.baidowi@its.ac.id

Sunarsih, Department of Marine Engineering Institut Teknologi Sepuluh Nopember ITS, Surabaya 60111, Indonesia.  
Email: sunarsih@its.ac.id

experiments, a simulation test was carried out with the resulting from the attachment of biofouling in the flat plate experiment.

After obtaining data from the flat plate simulation, regression analysis was performed on the simulation

help of Fine Marine to find the amount of roughness results to obtain the increase in roughness due to biofouling attachment. The regression results showed the amount of roughness at 7, 12, 18, and 24 months.

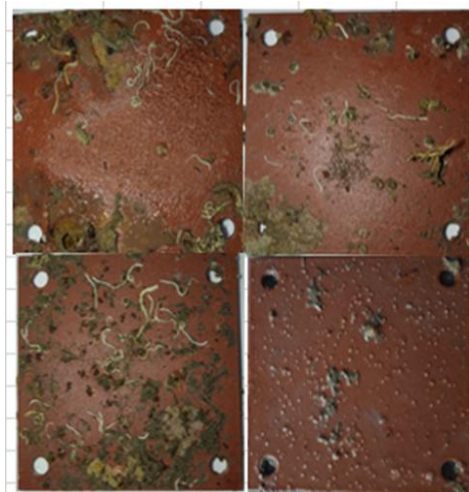


Figure. 1. Fouling conditions on test specimens [11]

TABLE 1.  
 SIMULATION RESULTS OF FLAT PLATE

Computation name	Froude	Month 7 Resistance (Kn)	Month 8 Resistance (Kn)	Month 9 Resistance (Kn)	Month 12 Resistance (Kn)
biokec01	0.1	0.00302885	0.00322881	0.00326405	0.00359498
biokec03	0.3	0.00302635	0.00322689	0.00326264	0.00359251
biokec05	0.5	0.00302544	0.00322615	0.00326209	0.00359146
biokec07	0.7	0.00302502	0.00322577	0.0032618	0.00359087
biokec09	0.9	0.00302473	0.00322556	0.00326163	0.00359051
biokec11	1.1	0.00302451	0.00322542	0.00326152	0.00359028
biokec13	1.3	0.00302425	0.00322532	0.00326143	0.0035901
AVERAGE		<b>0.003025593</b>	<b>0.003226274</b>	<b>0.003262166</b>	<b>0.00359153</b>

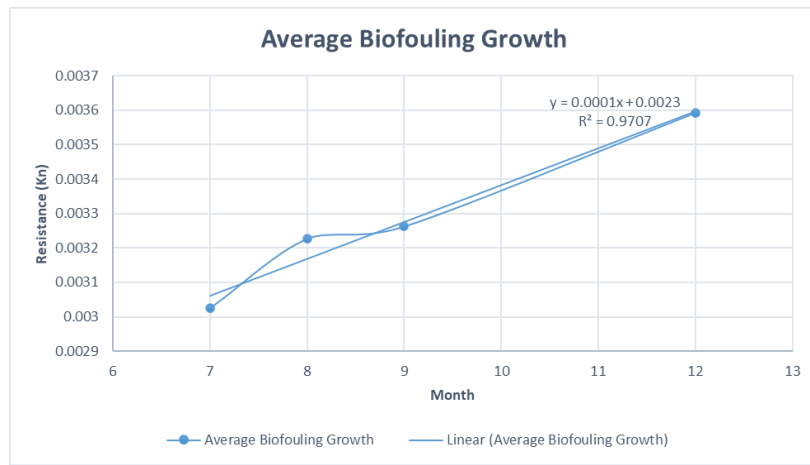


Figure. 2. Average biofouling growth chart

Based on the results of the biofouling growth experiment, the biofouling growth rate was modeled using the available growth regression graph. In this experiment, the regression equation obtained was:

$$Y = 0.0001x + 0.0023$$

From the following equation, biofouling growth can be predicted at 7, 12, 18, and 24 months as follows:

TABLE 2.  
PREDICTION OF BIOFOULING GROWTH RATE

MONTH	ROUGHNESS
7	0.00306
12	0.00360
18	0.00424
24	0.00488

#### B. Data Collection and Modeling

This study uses a 3-dimensional model of a tanker with the help of Maxsurf software made based on simulation

conditions as shown in Figure 2, where Figure 2 is a model with hull conditions that are evenly marketed throughout the underwater area (regular roughness).



Figure. 3. 3D model for regular roughness simulation

#### C. Geometrical Modeling, Meshing, and boundary conditions

This research uses a 3-dimensional model of the hull of the underwater area. Numerical simulation results in interpolation of boundary conditions values in the calculation process, so the results are wrong and divergence occurs in the calculation process due to the unrealistic calculation values in the boundary conditions. Divergence is the opposite of convergence and if a simulation the results can be trusted if it reaches the value of convergence. Convergence can be said if the residual or conservation measure of fluid characteristics as a whole gets a very small value [13]. However, there are other things that become parameters in the accuracy of numerical simulation results, namely in CFD simulations to define boundary conditions that can accurately describe the problem in order to get the desired simulation results. Boundary conditions are

boundary conditions in the form of geometry in numerical simulations [1].

The domain is created by defining a box around the ship, and the size of the computational domain is based on the length of the ship. Due to symmetry, only half of the ship is simulated. The boundary conditions of the computational domain as seen in Figure 2. are as follows, The inlet is located at 2.0 L upstream of the ship. The outlet is located at 4.0 L behind the ship. The side wall is located at 1.5 L beside the ship, where L is entirely at the waterline. The boundary conditions at the inlet, outlet, and side walls are all set as the free-flow far-field velocity. The bottom and top walls are located at 1.50 L below the ship and 1.5 L above the ship, respectively, where the boundary conditions are defined as the specified pressure. The boundary conditions on the hull are specified as wall function, where the wall function is given a certain roughness. Furthermore, heave and pitch motions are solved in the simulation.

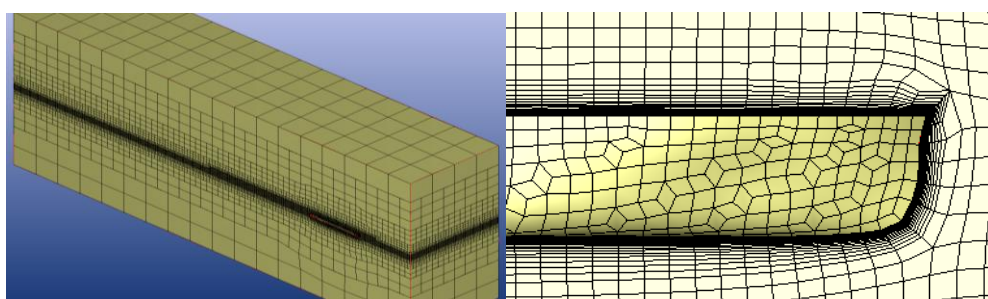


Figure. 4. Computational domain with the ship model in it (left) and mesh of the hull form (right)

#### D. Grid independence tests

To determine the optimum grid size (number of cells) and to investigate the convergence of numerical solutions, tests were conducted such that the numerical results met the grid-independence criteria. In these tests,

the total ship resistance coefficient  $C_r$  was calculated using an increasing number of cells in the simulation. The number of cells in the last simulation of the next two simulations was approximately double that of the previous simulation. The percentage error was

determined to measure the difference in Cr between the last and previous simulations. The results are tabulated in

Table 3 and visualized in Figure 5.

TABLE 3.  
 GRID INDEPENDENCE TESTS

NO	MESS/CELL	DIFFERENCE (%)
1	937230	0%
2	949602	1.31%
3	959585	1.05%
4	963022	0.36%
5	998117	3.58%
6	1006967	0.88%
7	1029451	2.21%

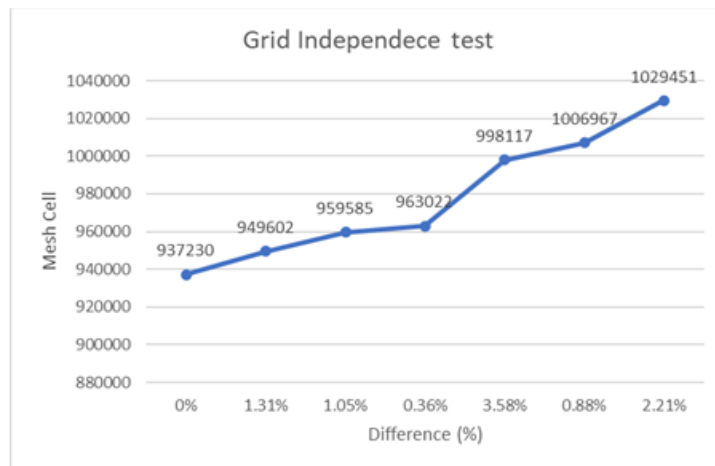


Figure. 5. Grid Independence Test

### III. RESULTS AND DISCUSSION

#### A. Umum

The Analysis and Discussion chapter is a chapter where the data obtained is processed or analyzed and then calculated and discussed. In accordance with the problem formulation described earlier, this Analysis and Discussion will analyze and discuss the effect of cleaning the underwater area of a ship's hull. This data analysis explains the results of research from several simulation variations, both from the results of simulations from regular roughness models and irregular roughness models with variations in roughness and speed of 10, 12, and 14 knots.

#### B. Analysis of the Efficient Time Period for cleaning the underwater area

##### 1. Analysis of No Fouling hulls with hulls from the 7th period

Figure. 6. is a graph comparing the results of the clean hull simulation with the hull in the 7th period. It can be seen that there is an increase in resistance when comparing the clean hull condition with the hull condition in the 7th period, with the largest increase at a speed of 12 knots with a percentage increase of 8.6% and the lowest increase in resistance at a speed of 14 knots with a percentage increase of 0.6%. Meanwhile, the average increase in resistance in the 7th period is 3.9%.'



**Figure. 6.** Comparison chart of No Fouling hull resistance with the 7th period

TABLE 4.  
 COMPARISON OF NO FOULING BOWL RESISTANCE WITH THE 7TH PERIOD

Speed (Knot)	Speed [m/s]	Froude	Period 7 Resistance (Kn)	No Fouling Resistance (Kn)	Difference (%)
10	5.14	0.161	56104.5	54614.4	2.7%
12	6.17	0.193	94211.5	86150	8.6%
14	7.2	0.226	144422	143626	0.6%
<b>AVERAGE</b>					<b>3.9%</b>

*2. Analysis of the hull of the No Fouling ship with the hull of the 12th period ship*

Figure 7 is a graph comparing the results of the clean hull simulation with the hull in the 12th period. It can be seen that there is an increase in resistance when comparing the clean hull condition with the hull

condition in the 12th period, with the largest increase at a speed of 12 knots with a percentage increase of 7.2% and the lowest increase in resistance at a speed of 14 knots with a percentage increase of 1.3%. Meanwhile, the average increase in resistance in the 12th period is 4.6%.

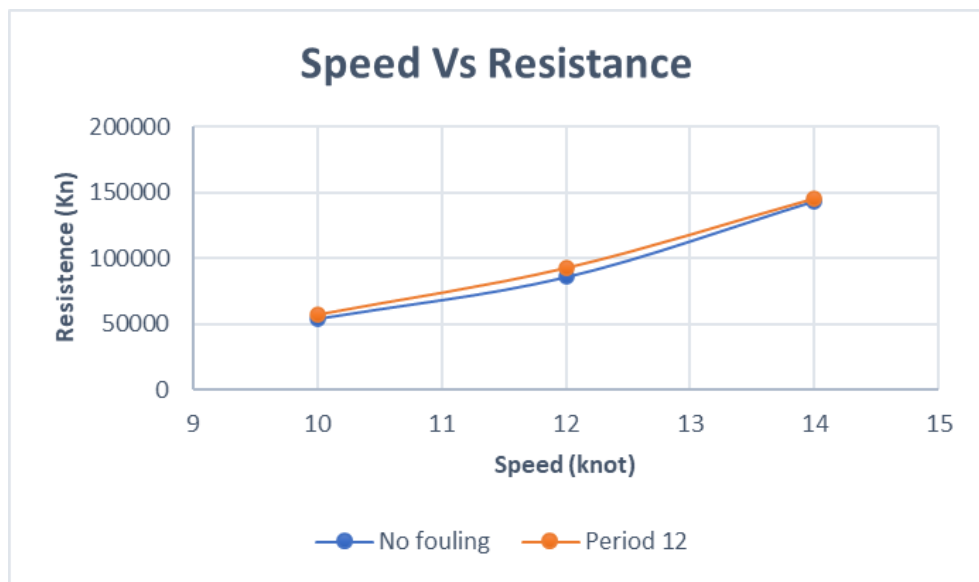


**Figure. 7.** Comparison chart of fouling-free hull resistance with the 12th period

TABLE 5.  
 COMPARISON OF NO FOULING BOWL RESISTANCE WITH THE 12TH PERIOD

Speed (Knot)	Speed [m/s]	Froude	Period 12 Resistance (Kn)	No Fouling Resistance (Kn)	Difference (%)
10	5.14	0.161	57634.7	54614.4	5.2%
12	6.17	0.193	92966.8	86150	7.3%
14	7.2	0.226	145486	143626	1.3%
<b>AVERAGE</b>					<b>4.6%</b>

*3. Analysis of the hull of the No Fouling ship with the hull of the 18th period ship*

Figure. 8. is a graph comparing the results of the clean hull simulation with the hull in the 18th period. It can be seen that there is an increase in resistance when comparing the clean hull condition with the hull

condition in the 18th period, with the largest increase at a speed of 12 knots with a percentage increase of 10.5%, while the lowest increase in resistance is at a speed of 14 knots with a percentage increase of 1.6%. Meanwhile, the average increase in resistance in the 18th period is 5.8%.



Figure. 8. Comparison chart of fouling-free hull resistance with the 18th period

TABLE 6.  
 COMPARISON OF NO FOULING BOWL RESISTANCE WITH THE 18TH PERIOD

Speed (Knot)	Speed [m/s]	Froude	Period 18 Resistance (Kn)	No Fouling Resistance (Kn)	Difference (%)
10	5.14	0.161	57713.9	54614.4	5.4%
12	6.17	0.193	96265.5	86150	10.5%
14	7.2	0.226	145992	143626	1.6%
<b>AVERAGE</b>					5.8%

4. Analysis of the hull of the No Fouling ship with the hull of the 24th period ship

Figure. 9. shows a comparison graph of the simulation results for a clean hull and a hull in the 24th period. It can be seen that there is an increase in resistance when comparing the clean hull condition with

the hull condition in the 24th period, with the largest increase at a speed of 12 knots with a percentage increase of 12.1%. The lowest increase in resistance is at speeds of 10 knots and 14 knots, with an increase of 1.1%. The average increase in resistance in the 24th period is 6.5%.



Figure. 9. Comparison chart of fouling-free hull resistance with the 24th period

TABLE 7.  
 COMPARISON OF NO FOULING BOWL RESISTANCE WITH THE 24TH PERIOD

Speed (Knot)	Speed [m/s]	Froude	Period 24 Resistance (Kn)	No Fouling Resistance (Kn)	Difference (%)
10	5.14	0.161	58315.3	54614.4	6.3%
12	6.17	0.193	98030	86150	12.1%
14	7.2	0.226	145260	143626	1.1%
<b>AVERAGE</b>					6.5%

The most efficient timing for underwater hull cleaning is determined by the increase in resistance. In periods 7 and 12, there was a relatively small increase in resistance of 0.7%, while in periods 12 and 18, there was an increase in resistance of 1.2%. In periods 18 and 24, there was an increase of 0.7%. From the above

conditions, it can be concluded that the largest increase in resistance occurred in the 18th period, with an average increase of 5.8%. Therefore, the most effective time to perform underwater hull cleaning is in the 18th period. Performing underwater hull cleaning in the 18th period can save fuel consumption by up to 5.8%.



Figure. 10. Graph of resistance increase in each period

TABLE 8.

RESUME AVERAGE INCREASE IN RESISTANCE

MONTH	AVERAGE	DIFFERENCE
7	3.9%	0%
12	4.6%	0.7%
18	5.8%	1.2%
24	6.5%	0.7%

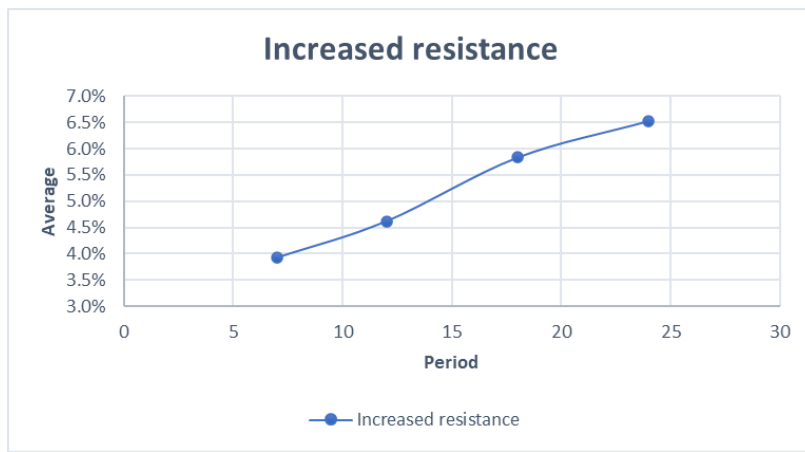


Figure. 11. Graph of the average increase in resistance

#### IV. CONCLUSION

Based on the results of the analysis and discussion, several conclusions can be drawn, namely

1. Based on the simulation of the experimental results conducted by Singgih (2022), biofouling growth was found to be 2-3%/month.
2. From the analysis obtained from the CFD simulation results, the total resistance on the ship's hull increased the most in the 24th period with an average increase of 12.1%.

3. From the analysis results, it can be concluded that the most efficient period for cleaning the underwater hull area is every 18 months of sailing after dry docking, with a reduction in fuel consumption of up to 5.8%.

#### ACKNOWLEDGEMENTS

The author would like to thank all individuals and institutions who indirectly supported this research through access to data, facilities, and academic feedback

REFERENCES

- [1] G. O. A study into the techniques needed to accurately predict skin friction using RANS solvers with validation against Froude's historical flat plate experimental data Date and Turnock 1999. (1999). J.C.Date and S.R. Turnock.
- [2] Al-Muhanna, K., & Habib, K. (2016). Marine bio-fouling of different alloys exposed to continuous flowing fresh seawater by electrochemical impedance spectroscopy. *Journal of Saudi Chemical Society*, 20(4), 391–396. <https://doi.org/10.1016/j.jscs.2012.07.008>.
- [3] Baital, Mum. S. (2016). Analisa Pengaruh Penempelan Marine Biofouling Terhadap Power Kapal Dengan Simulasi CFD.
- [4] Bertram, V. (2012). Practical Ship Hydrodynamics. Practical Ship Hydrodynamics. <https://doi.org/10.1016/C2010-0-68326-X>.
- [5] Callow, J. A., & Callow, M. E. (2011). Trends in the development of environmentally friendly fouling-resistant marine coatings. In *Nature Communications* (Vol. 2, Issue 1). <https://doi.org/10.1038/ncomms1251>.
- [6] Demirel, Y. K., Turan, O., & Incecik, A. (2017). Predicting the effect of biofouling on ship resistance using CFD. *Applied Ocean Research*, 62, 100–118. <https://doi.org/10.1016/j.apor.2016.12.003>.
- [7] Demirel, Y. K., Uzun, D., Zhang, Y., Fang, H. C., Day, A. H., & Turan, O. (2017). Effect of barnacle fouling on ship resistance and powering. *Biofouling*, 33(10), 819–834. <https://doi.org/10.1080/08927014.2017.1373279>.
- [8] Egan, S. (2001). Production and regulation of fouling inhibitory compounds by the marine bacterium *Pseudoalteromonas tunicata*.
- [9] Kim, D. H., Alayande, A. B., Lee, J. M., Jang, J. H., Jo, S. M., Jae, M. R., Yang, E., & Chae, K. J. (2024). Emerging marine environmental pollution and ecosystem disturbance in ship hull cleaning for biofouling removal. In *Science of the Total Environment* (Vol. 906). Elsevier B.V. <https://doi.org/10.1016/j.scitotenv.2023.167459>.
- [10] Naval Sea Systems Command. (2006). Waterborne underwater hull cleaning of navy ships. *Naval Ships' Technical Manual*, 68pp.
- [11] Pribadi, Singgih. (2022). Studi Eksperimen Pertumbuhan Biofouling Terhadap Spesimen Uji yang Tidak Bergerak. ITS Surabaya.
- [12] Uzun, D., Demirel, Y. K., Coraddu, A., & Turan, O. (2019). Time-dependent biofouling growth model for predicting the effects of biofouling on ship resistance and powering. *Ocean Engineering*, 191(June), 106432. <https://doi.org/10.1016/j.oceaneng.2019.106432>.
- [13] Versteeg, H. K., & Malalasekera, W. (n.d.). *An Introduction to Computational Fluid Dynamics* Second Edition. [www.pearsoned.co.uk/versteeg](http://www.pearsoned.co.uk/versteeg).
- [14] Zhong, X., Dong, J., Liu, M., Meng, R., Li, S., & Pan, X. (2022). Experimental study on ship fouling cleaning by ultrasonic-enhanced submerged cavitation jet: A preliminary study. *Ocean Engineering*, 258. <https://doi.org/10.1016/j.oceaneng.2022.111844>.